行政院國家科學委員會專題研究計畫成果報告

雙電子游離化產生多光子過程之研究

計畫類別：☐ 個別型計畫　　☐ 整合型計畫

計畫編號：NSC 88-2112-M-009-013

執行期間：87 年 8 月 1 日至 88 年 7 月 31 日

個別型計畫：計畫主持人：韓建珊

處理方式：☐ 可立即對外提供參考
☐ 一年後可對外提供參
☐ 兩年後可對外提供參考
(必要時，本會得展延發表時限)

執行單位：國立交通大學電子物理系

中華民國 89 年 1 月 28 日

Abstract

We present a theoretical investigation on the above-threshold ionization of the exited hydrogen atom in (ns) states using a non-perturbative method of solving the Schrodinger equation in momentum space. A systematic calculation on the photo-electron energy spectra is performed, and the dependence of the spectra on the laser field strength and frequency is also discussed.

Key words: non-perturbative theory, multiphoton ionizatino

中文摘要

我們以非微擾理論研究激發氫原子在(ns)態時產生多光子之離化過程，我們對其過程中產生之光電子能譜作一有系統性的計算，並討論此能譜與雷射之強度和頻率的關係，以對此過程獲得較深入的瞭解。

關鍵詞：非微擾理論、多光子之離化過程

I. Introduction

The above-threshold ionization (ATI) of atoms in the intense radiation field exhibits many interesting nonlinear features that have attracted a great deal of investigations both experimentally and theoretically. A review on this subject can be found in the article by Burnett et. al.[1]. One of the most important nonlinear effects in ATI is the significant suppression of the lowest-order peaks in the photoelectron energy spectra with increased laser intensity. Another striking feature in ATI is that the relative sizes of the consecutive peaks in the spectra become inverted. This "peak-switching" effect is caused by the multiple transitions of the electron through the continua during the redistribution of the final continuum states. Most of the theoretical studies on ATI are concentrated on the hydrogen atom in the ground state[2-14]. For the excited hydrogen atom, the investigation is less explored. The two-photon ionization cross-sections with one photon above threshold for hydrogen atom in the excited (ns) states have been studied by Aymar and Crance[15] using a method based on numerical computations in the frame work of the central field approximation, and also by Karule[16] employing above threshold analytic continuation of the Sturmian expansion for the transition matrix elements. The problem was further extended to the three-photon ionization with two-photon above threshold by Han and Yaung[17] using a Monte Carlo approach. Recently, a number of interests are concerning for the highly excited hydrogen atom in an intense field using semi-classical approach, and the quantum-classical correspondence is discussed[18,19]. In the previous work[11], we applied a non-perturbative method of solving the Schrödinger equation in momentum space to investigate the above threshold ionization of the hydrogen atom in the ground state. In the present paper, we shall extend our analysis to the excited hydrogen atom in the (ns) states and perform a systematic calculation for the photoelectron energy spectra. We find that quite different results are obtained when the hydrogen atom in the higher excited (ns) state undergoes many photon ionizations. The mechanism for this different behavior will be discussed.

II. Theory

The method used in this paper has been developed in the previous works[11,20]. We briefly review the essential features here. Consider an electron initially, at $t = 0$, bounded by the atomic potential, V, in the state $|\Phi_n(t)\rangle = |\phi_n\rangle exp(-iE_i t/\hbar)$, with E_i the initial energy. The time-dependent wave function, $|\Psi(t)\rangle$, is expanded in terms of the Volkov functions[21] and substituted into the time-dependent Schrödinger equation that leads to a set of first-order inhomogeneous integrodifferential equations for the expansion coefficient $a_{\vec{k}}(t)$. A slowly-varying function $b_{\vec{k}}(t)$ is extracted and we can extrapolate it using a Taylor series expansion. For the monochromatic linearly-polarized field

$$\vec{A}(t) = \vec{A}_0 coswt, \tag{1}$$

the ionization amplitude can be obtained, in the first-order approximation, as

$$\begin{aligned} a_{\vec{k}}(t) &= a_{\vec{k}}(0) - \frac{i}{\hbar}\sum_n J_n(\xi) b_{\vec{k}}(0) \\ &\times \int_0^t dt' exp\left[\frac{i}{\hbar}\left(\frac{p^2}{2m} - E_i - Q - n\hbar w\right)t'\right] \end{aligned} \tag{2}$$

where $a_{\vec{k}}(0)$ is determined from the initial boundary condition and the coupling parameter $\xi = \frac{e}{mcw}(\vec{k}\cdot\vec{A}_0)$. The quantity Q is given as

$$Q = \frac{1}{b_{\vec{k}}(0)}\int d\vec{k}'[\dot{F}_{\vec{k}'}(0)a_{\vec{k}'}(0) + b_{\vec{k}'}(0)]\langle\vec{k}|V|\vec{k}'\rangle, \tag{3}$$

with

$$F_{\vec{k}}(t) = \left(\frac{\hbar^2 k^2}{2m} - E_i\right)t - \frac{e\hbar(\vec{k}\cdot\vec{A}_0)}{mcw} sinwt, \tag{4}$$

and $|\vec{k}\rangle$ is the eigenvector of $\vec{p}$. Eq.(2) shows that the ATI photoelectron peaks occur at energies

$$E_k = \frac{p^2}{2m} = n\hbar w - I_i + Q \tag{5}$$

where $I_i = -E_i$ is the ionization energy for the initial state ϕ_i. It can be seen from eq.(5) that the energies are shifted by an amount Q, which comes from the $\vec{A} \cdot \vec{p}$ interaction and is an important effect responsible for the peak-switching in the photoelectron spectra.

III. Result and Discussion

We now present the numerical calculation of the above-threshold ionization for the hydrogen atom in the excited (ns) states. We have calculated the probability function, $|a_k(t \to \infty)|^2$, for different values of the laser field strength and laser frequency. The expression for $|a_k(t \to \infty)|^2$ can be easily obtained from eq.(2) by letting $t \to \infty$. We first consider the case of (2s) state. Figure 1 shows the photoelectron spectra for the laser frequency $w = 0.05$ a.u. ($N_0 = 3$), where N_0 is the minimum number of photons absorbed required for ionization. It is clearly seen that the lowest-order peak is significantly suppressed with increased laser field. Our results also exhibit the peak-switching, i.e., the magnitudes of consecutive peaks become inverted as the field increases. Similar results are obtained for the cases of laser frequencies $w = 0.03$ a.u. ($N_0 = 5$) and $w = 0.02$ a.u. ($N_0 = 7$). These important features can be seen more qualitatively in the plot of the probability function versus the field intensity I for different photons absorbed as shown in Fig.2. In general, for low field region, the curves increase linearly with the field strength. As the laser field increases, the higher-order curves increase rapidly and eventually overcome the lower-order ones. Thus, the peak-switching will occur successively at some critical field for higher-order curves, and the curves are finally all reversed in the high field region. It is found that the peak-switching occurs in the field ranges $I = 8 \times 10^{11} \sim 6 \times 10^{13} (W - cm^{-2})$ for the case $w = 0.05$ a.u., $I = 7 \times 10^{10} \sim 9 \times 10^{12} (W - cm^{-2})$ for $w = 0.03$ a.u. and $I = 2 \times 10^{10} \sim 6 \times 10^{12} (W - cm^{-2})$ for $w = 0.02$ a.u.. The reason for this is due to the energy shift Q, which is an important effect responsible for the peak-switching as we shall discuss later. We have also studied the above-threshold ionization for (3s) and (4s) states. The results are shown in Figs.3 and 4, respectively. For (3s) state, the peak-inversions again occur gradually as the field increases to higher values for the cases of high frequencies $w = 0.022$ a.u. ($N_0 = 3$) and $w = 0.0135$ a.u. ($N_0 = 5$) as shown in Figs.(3a) and (3b). However, we find a quite different result as the laser frequency decreases to lower values, that is, for many-photon ionization. It can be seen in Fig.3(c) that for $w = 0.0092$ a.u. ($N_0 = 7$), the order of curves changes very rapidly and becomes all reversed abruptly in a very short field region: $I = 2 \times 10^{10} \sim 8 \times 10^{10}(W - cm^{-2})$. This dramatic behavior is also observed for the case of (4s) state as shown in Figs.4(b) and 4(c), where for the low frequencies $w = 0.0075$ a.u. ($N_0 = 5$) and $w = 0.005$ a.u. ($N_0 = 7$), the peak-inversions again occur in very short field regions : $I = 1 \times 10^{11} \sim 7 \times 10^{11}(W - cm^{-2})$ for the case of $w = 0.0075$ a.u., and $I = 2 \times 10^{10} \sim 8 \times 10^{10}(W - cm^{-2})$ for $w = 0.005$ a.u.. The reason for this is due to the effect of the energy shift as we just pointed out. In the following, we shall discuss the relationship of the energy shift Q with the peak-switching observed in Figs.2-4.

Figure 5 shows the result of the energy shift Q as a function of the field intensity I for the (2s) state. For small field Q is small, so the lower-order spectra are dominant and no peak-switching occurs. But for higher field Q increases fast and its effect becomes sizable. The peak-switching will then occur successively for each higher-order curve at some critical field as shown in Fig.2. It is worth noting that our energy shifts Q, which come from the $\vec{A} \cdot \vec{p}$ interaction, are different from different final states. This differs from some previous calculations where the shifts are due to the ponderomotive energy, which increases only with the field strength, but remains the same for all states. However, our energy shift Q increases not only with the field, but also with the final continuum states. As seen from Fig.5, at a fixed I the tendency of the magnitude of Q to increase with the order of curves is quite fast.

Therefore, these two effects of increasing Q are combined together to enhance the interesting results obtained in Fig.2. We have also studied the cases of (3s) and (4s) states with the results shown in Figs. 6 and 7, respectively. It can be seen that for high laser frequencies $w = 0.022$ a.u. ($N_0 = 3$) and $w = 0.0135$ a.u. ($N_0 = 5$) of (3s) state in Figs.6(a) and 6(b) , and $w = 0.015$ a.u. ($N_0 = 3$) of (4s) state in Fig.7(a), Q increases gradually with the field strength as in the case of (2s) state, so the occurrence of the peak-switching is similar for all the cases of (2s), (3s) and (4s) states as indicated in Figs. 2-4. However, the situation becomes quite different when the laser frequency becomes small. It is clearly seen that for $w = 0.0092$ a.u. ($N_0 = 7$) of (3s) state in Fig.6(c), and $w = 0.0075$ a.u. ($N_0 = 5$) and $w = 0.005$ a.u. ($N_0 = 7$) of (4s) states in Figs.7(b) and 7(c), Q increases abruptly in a very short field region: $I = 2 \times 10^{10} \sim 8 \times 10^{10}(W - cm^{-2})$ for the case of $w = 0.0092$ a.u. ($N_0 = 7$) of (3s) state and for $w = 0.005$ a.u. ($N_0 = 7$) of (4s) state. This abrupt change in Q is also observed for the case of $w = 0.0075$ a.u. ($N_0 = 5$) of (4s) state in the field region: $I = 1 \times 10^{11} \sim 7 \times 10^{11}(W - cm^{-2})$. Thus, the effect of Q increases so rapidly that the peak-inversions will also occur abruptly in these corresponding short field regions as we have pointed out before in Figs. 3 and 4. Therefore, our results show that the energy shift Q is closely related to the peak-switching in the photoelectron spectra, and the correspondence between them is quite consistent.

IV. Conclusion

We have presented a systematic calculation on the above-threshold ionization for the excited hydrogen atom in the (ns) states. We have calculated the photoelectron energy spectra for different field strengths and laser frequencies. It is found that the peak-switching in the spectra is closely related to the energy shift Q. For the (2s) state, Q is small for small field strength, and the lower-order spectra dominates so that no peak-switching occurs. As the field strength increases, the energy shift Q gradually increases so the peak-switching will occur successively for each higher-order curve at some critical field. For the (3s) and (4s) states, the behaviors of the energy shift Q and the peak-switching are similar to the (2s) state when the laser frequency is high. However, we find a quite different result for the case of low frequencies, that is, for many-photon ionizations. It is found that Q increases abruptly in a very short field region so that the peak-switching will occur very rapidly, and the order of curves becomes all reversed in this corresponding field region.

Reference:

1. K. Burnett, V.C. Reed, and P.L. Knight, J. Phys. B26,561(1993).

2. S.I. Chu and J. Cooper, Phys. Rev. A32,2769(1985).

3. Y. Gontier, N.K. Rakman, and M. Trahin, Phys. Rev. A34,1112(1986).

4. K.C. Kulander, Phys. Rv. A35,445(1987).

5. R.M. Potvliege and R. Shakeshaft, Phys. Rev. A38, 1098(1988).

6. X. Tang, H. Rudolph, and P. Lambropoulos, Phys. Rev. lett. 65,3269(1990).

7. M. Pont and M. Gavrila, Phys. Rev. Lett. 65,2362(1990).

8. M. Horbatsch, J. Phys. B24, 4919(1991).

9. B. Piraux, E. Huens, and P.L. Knight, Phys. Rev. A44,721(1991).

10. J.L. Krouse, K.J. Schafer, and K. Kulander, Phys. Rev. A45,4998(1992).

11. C.S. Han, J. Phys. B27,5707(1994).

12. R.A. Blank and M. Shapiro, Phys. Rev. A50,3234(1994).

13. S. Dionissopoulou, Th. Mercouris, A. Lyras, Y. Komninos, and C.A. Nicolaides, Phys. Rev. A51,3104(1995).

14. J.Z. Kaminski, A. Jaron, and F. Ehlotzky, Phys. Rev. A53,1756(1996).

15. M. Aymar and M. Crance, J. Phys. B13,L287(1980).

16. E. Karule, J. Phys. B18,2207(1985).

17. C.S. Han and J.C.I. Yaung, J. Phys. B23,615(1991).

18. D. Richards, J. Phys. B25,1347(1992).

19. D. Richards and T. Szeredi, J. Phys. B28,L413(1995).

20. C.S. Han, J. Phys. B23,L495(1990).

21. D.M. Volkov, Z. Phys. 94,250(1935).

Figure captions

Fig.1 Relative heights of ATI peaks, normalized to the first peak for the (2s) state of hydrogen atom. The laser frequency is $w = 0.05$ a.u. ($N_0 = 3$) and the laser field strengths are (a) 0.001 a.u., (b) 0.005 a.u., (c) 0.01 a.u., (d) 0.05 a.u., (e) 0.1 a.u..

Fig.2 Probability density $P_k = |a_k(t \to \infty)|^2$ as a function of the field intensity $I(W - cm^{-2})$ for the (2s) state of hydrogen atom. The laser frequencies are (a)w=0.05 a.u. ($N_0 = 3$), (b) $w = 0.03$ a.u. ($N_0 = 5$), and (c) $w = 0.02$ a.u. ($N_0 = 7$). N is the total number of photons absorbed.

Fig.3 Same as in Fig.2, but for the (3s) state. The laser frequencies are (a) $w = 0.022$ a.u. ($N_0 = 3$), (b) $w = 0.0135$ a.u. ($N_0 = 5$), and (c) $w = 0.0092$ a.u. ($N_0 = 7$).

Fig.4 Same as in Fig.2, but for the (4s) state. The laser frequences are (a) $w = 0.015$ a.u. ($N_0 = 3$), (b) $w = 0.0075$ a.u. ($N_0 = 5$), and (c) $w = 0.005$ a.u. ($N_0 = 7$).

Fig.5 The energy shift Q as a function of the field intensity $I(W - cm^{-2})$ for the (2s) state of hydrogen atom. N in the total number of photons aborbed. The laser frequencies are (a) $w = 0.05$ a.u. ($N_0 = 3$); (b) w =0.03 a.u. ($N_0 = 5$), and (c) $w = 0.02$ a.u. ($N_0 = 7$).

Fig.6 Same as in Fig.5, but for the 3s state. The laser frequencies are (a) $w = 0.022$ a.u. ($N_0 = 3$), (b) $w = 0.0135$ a.u. ($N_0 = 5$), and (c) $w = 0.0092$ a.u. ($N_0 = 7$).

Fig.7 Same as in Fig.5, but for the 4s state. The laser frequencies are (a) $w = 0.015$ a.u. ($N_0 = 3$), (b) $w = 0.0075$ a.u. ($N_0 = 5$), and (c) $w = 0.005$ a.u. ($N_0 = 7$).

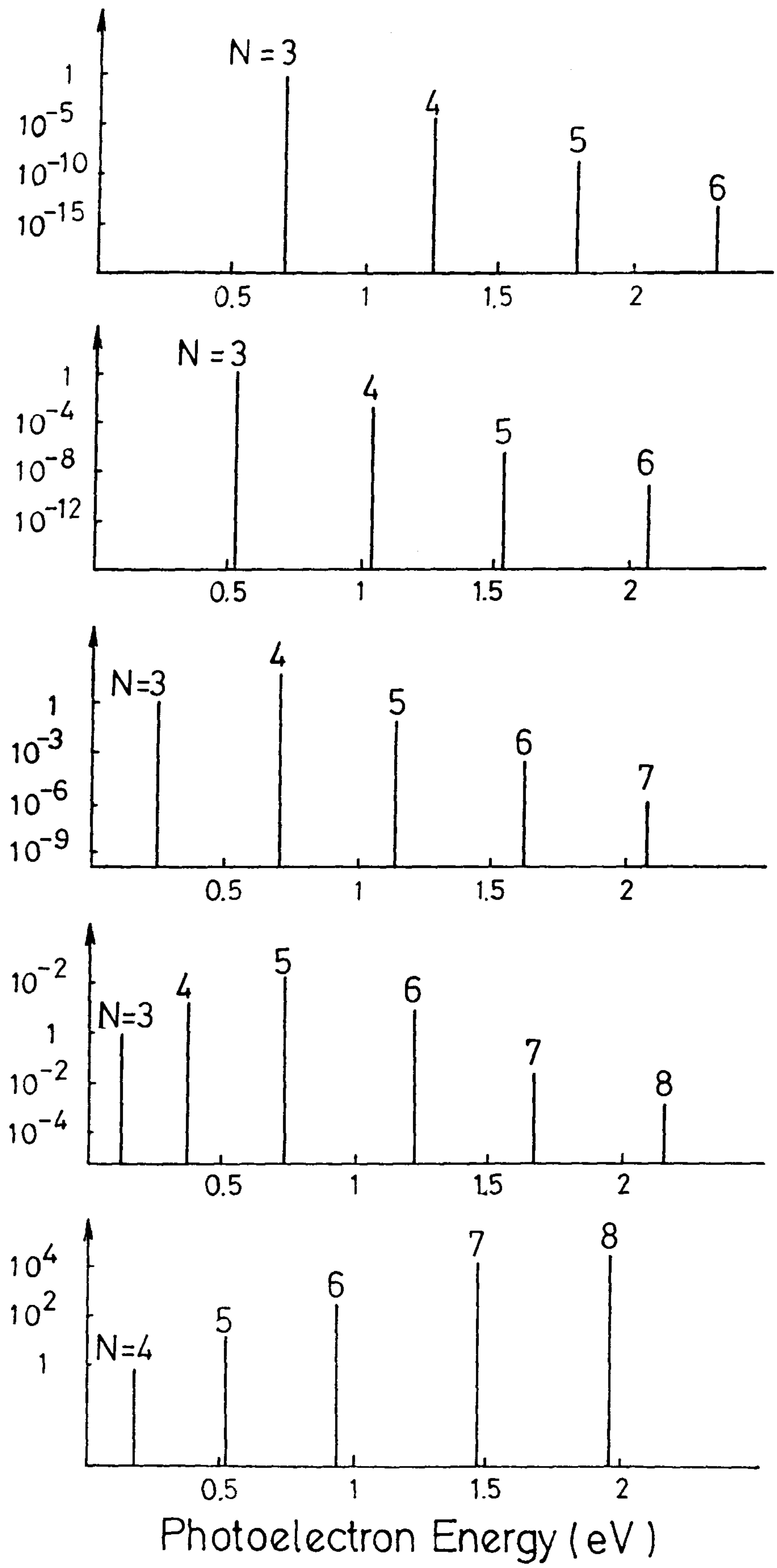

N = 3
4
5
6
1
10^-5
10^-10
10^-15
0.5
1
1.5
2
N = 3
4
5
6
1
10^-4
10^-8
10^-12
0.5
1
1.5
2
N=3
4
5
6
7
1
10^-3
10^-6
10^-9
0.5
1
1.5
2
N=3
4
5
6
7
8
10^-2
1
10^-2
10^-4
0.5
1
1.5
2
N=4
5
6
7
8
10^4
10^2
1
0.5
1
1.5
2
Photoelectron Energy (eV)

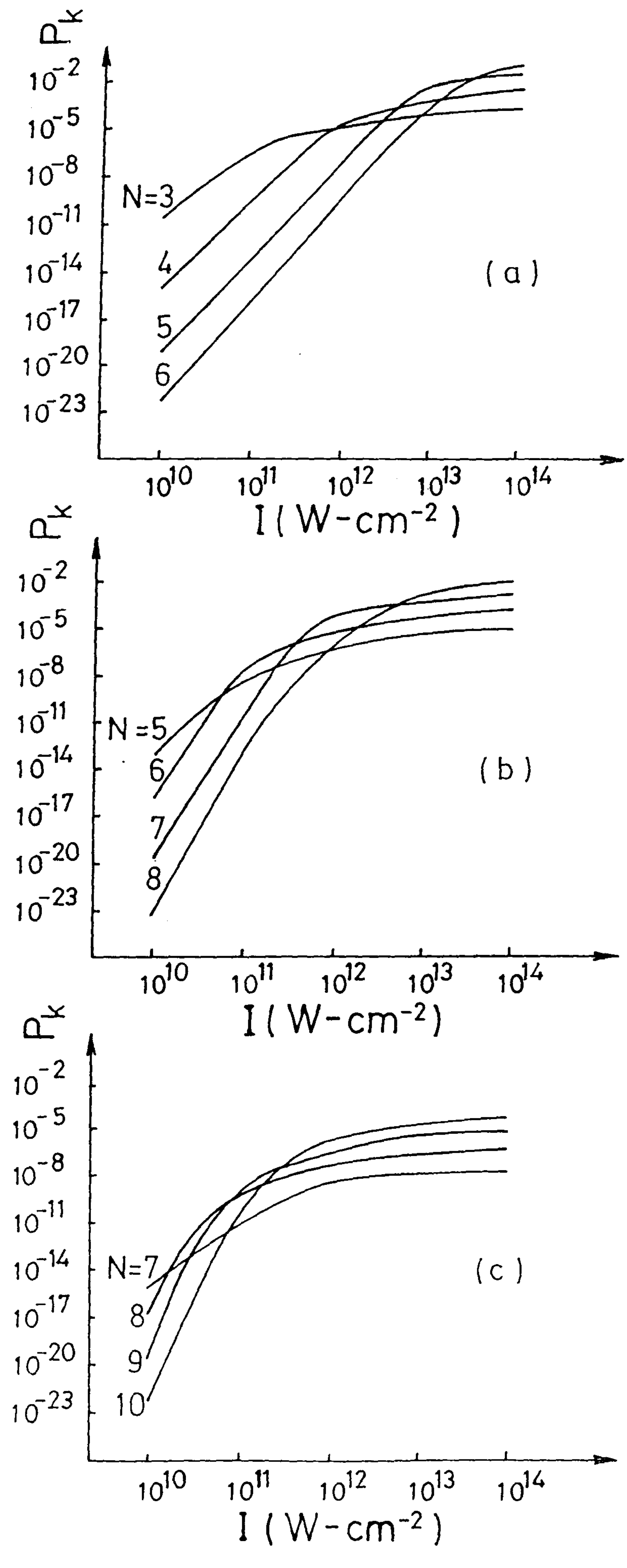

(a)
N=3
4
5
6
(b)
N=5
6
7
8
(c)
N=7
8
9
10
P_k
10^{-2}
10^{-5}
10^{-8}
10^{-11}
10^{-14}
10^{-17}
10^{-20}
10^{-23}
10^{10}
10^{11}
10^{12}
10^{13}
10^{14}
$I\ (W\text{-}cm^{-2})$

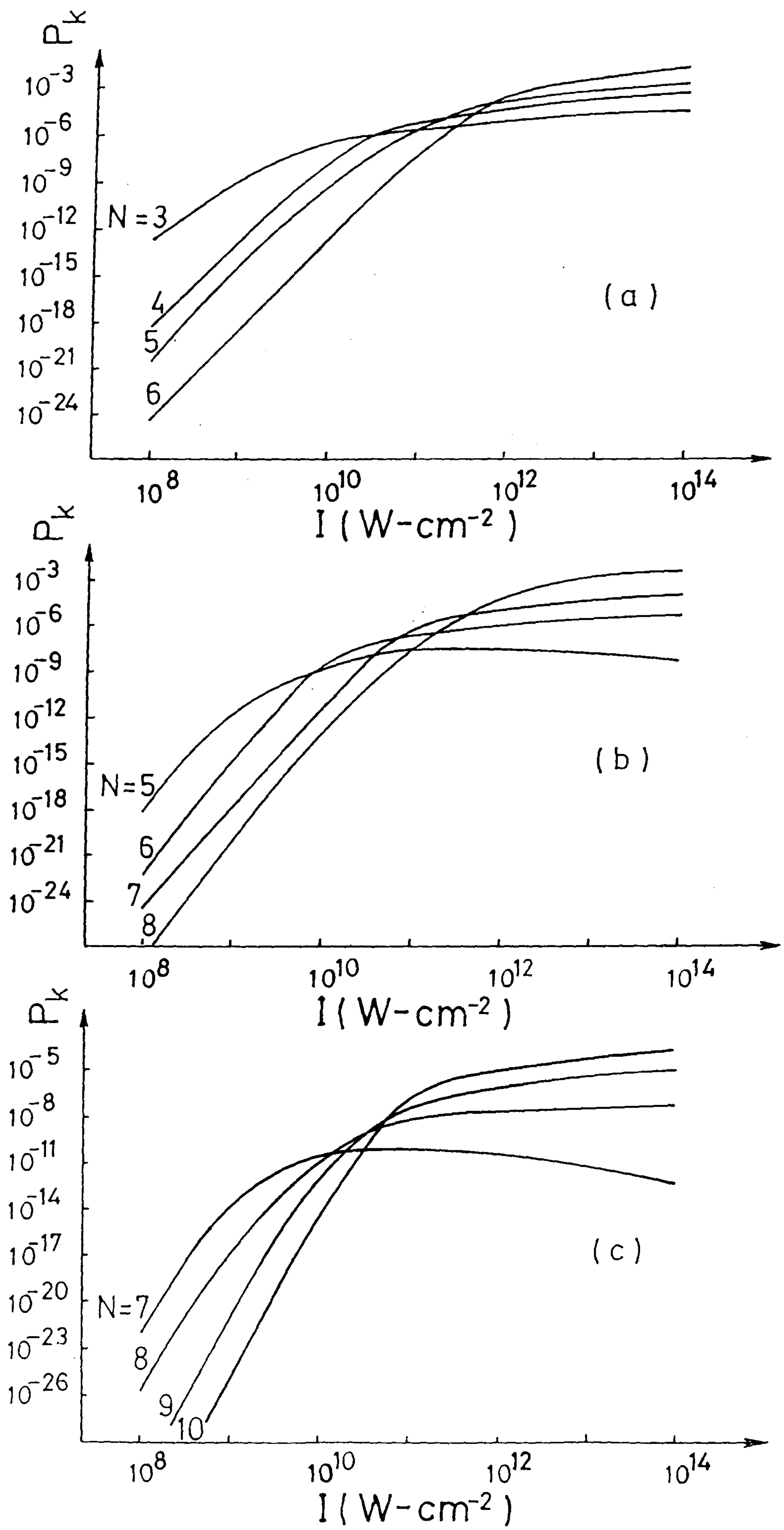
P_k
10^-3
10^-6
10^-9
10^-12
10^-15
10^-18
10^-21
10^-24
N = 3
4
5
6
(a)
10^8
10^10
10^12
10^14
I (W-cm^-2)
P_k
10^-3
10^-6
10^-9
10^-12
10^-15
10^-18
10^-21
10^-24
N=5
6
7
8
(b)
10^8
10^10
10^12
10^14
I (W-cm^-2)
P_k
10^-5
10^-8
10^-11
10^-14
10^-17
10^-20
10^-23
10^-26
N=7
8
9
10
(c)
10^8
10^10
10^12
10^14
I (W-cm^-2)

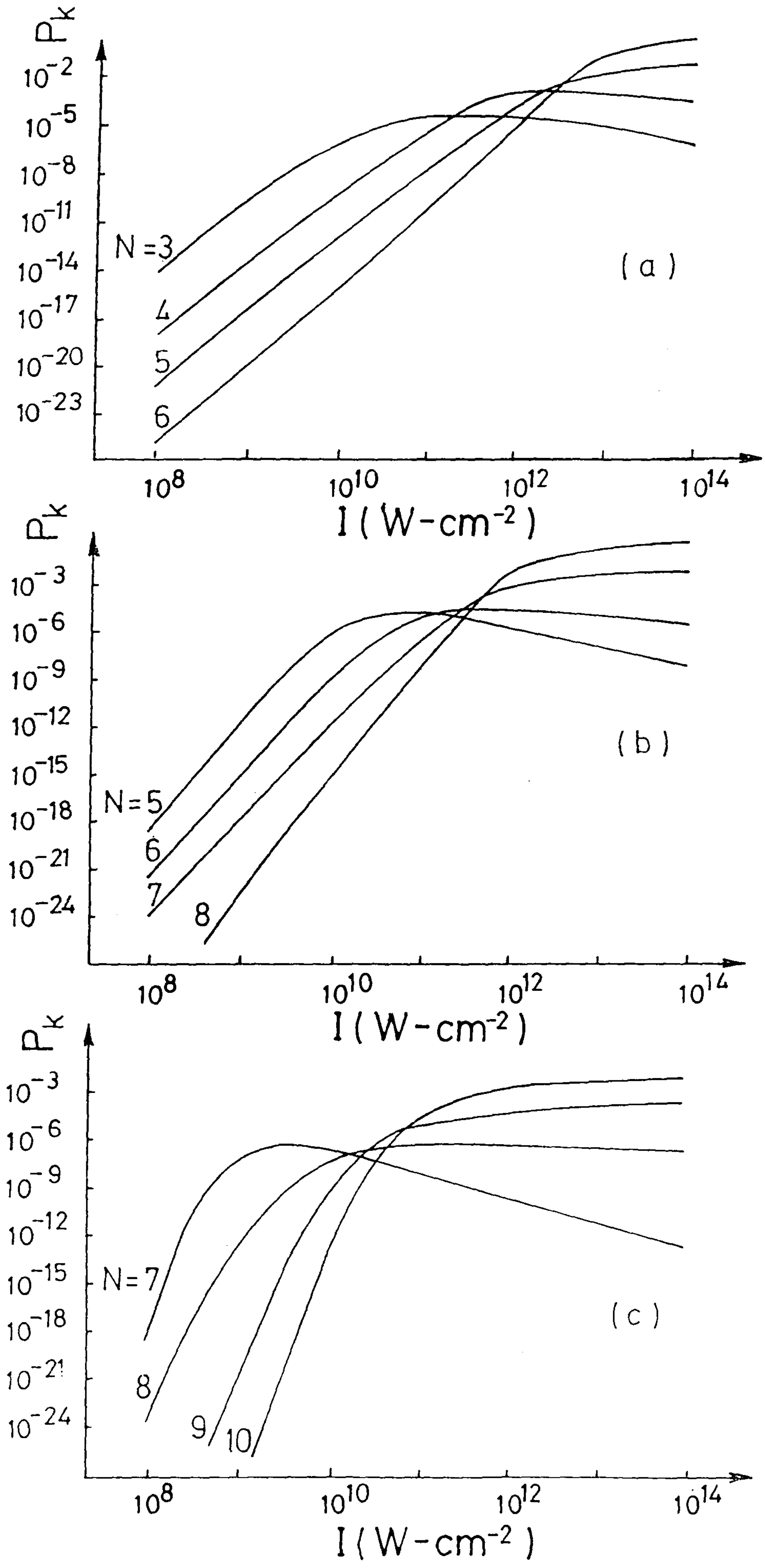

P_k
10^-2
10^-5
10^-8
10^-11
10^-14
10^-17
10^-20
10^-23
N=3
4
5
6
(a)
10^8
10^10
10^12
10^14
I (W-cm^-2)
P_k
10^-3
10^-6
10^-9
10^-12
10^-15
10^-18
10^-21
10^-24
N=5
6
7
8
(b)
10^8
10^10
10^12
10^14
I (W-cm^-2)
P_k
10^-3
10^-6
10^-9
10^-12
10^-15
10^-18
10^-21
10^-24
N=7
8
9
10
(c)
10^8
10^10
10^12
10^14
I (W-cm^-2)

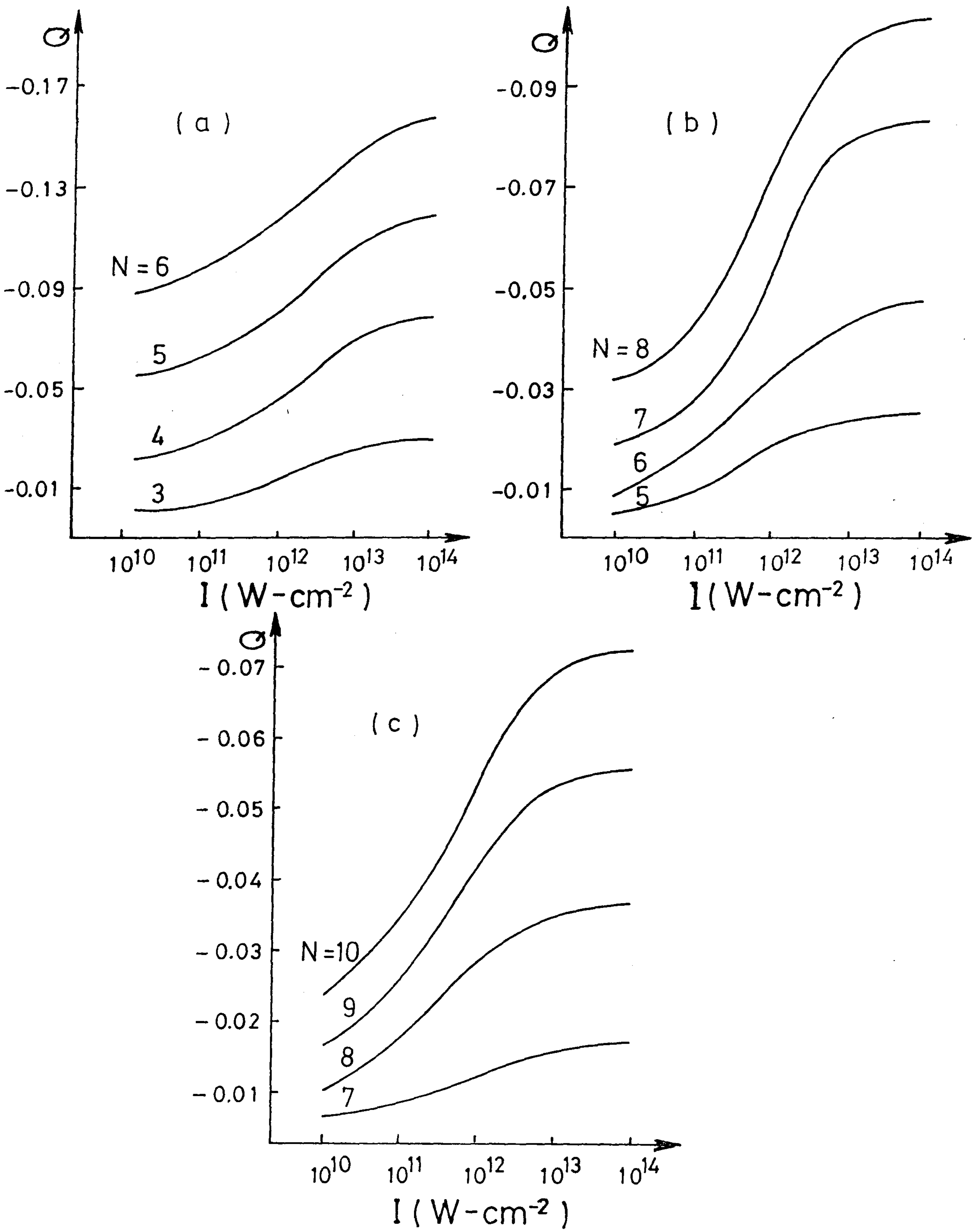

Q
-0.17
-0.13
-0.09
-0.05
-0.01
(a)
N = 6
5
4
3
10^10 10^11 10^12 10^13 10^14
I (W-cm^-2)
Q
-0.09
-0.07
-0.05
-0.03
-0.01
(b)
N = 8
7
6
5
10^10 10^11 10^12 10^13 10^14
I (W-cm^-2)
Q
- 0.07
- 0.06
- 0.05
- 0.04
- 0.03
- 0.02
- 0.01
(c)
N =10
9
8
7
10^10 10^11 10^12 10^13 10^14
I (W-cm^-2)

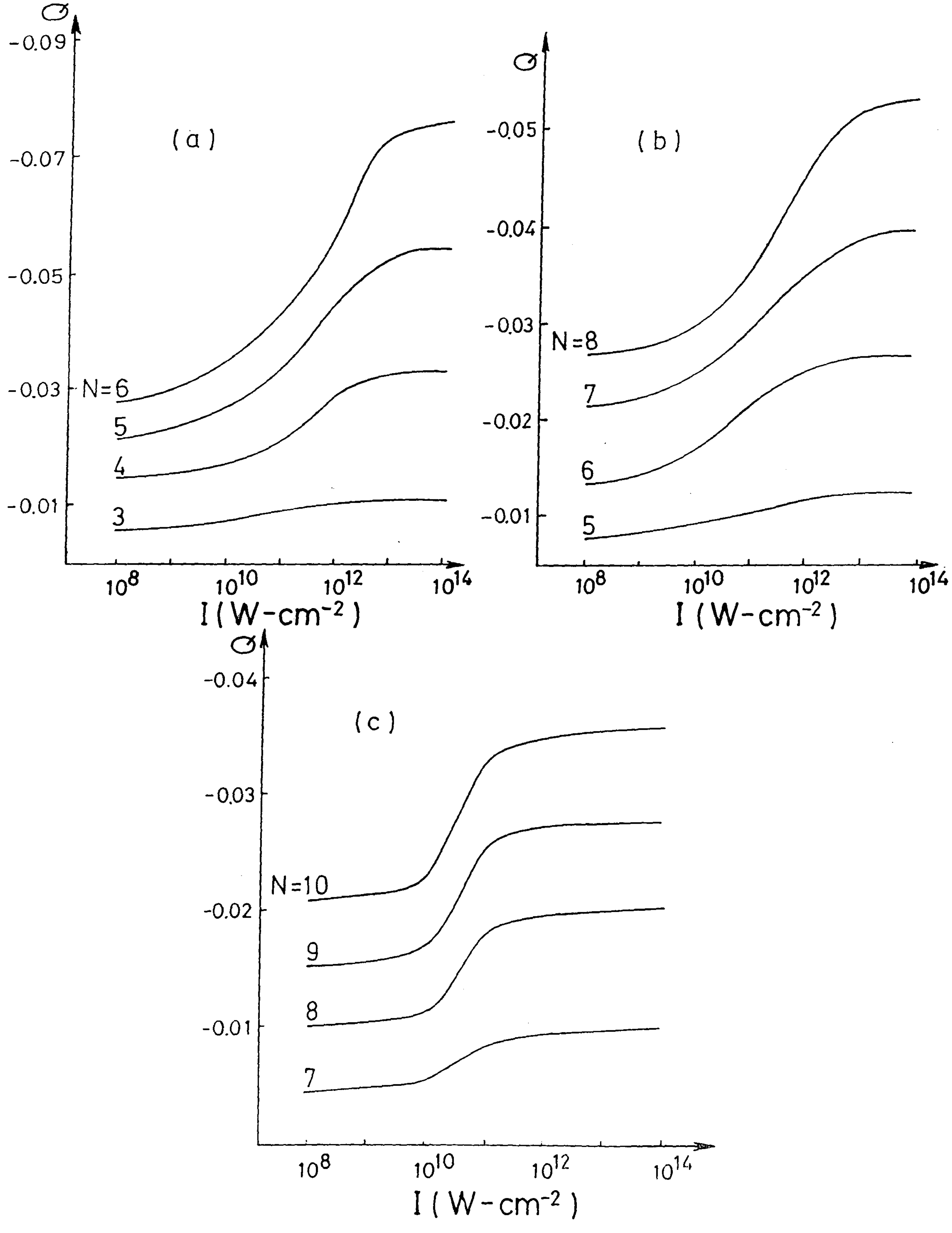

(a)
Q
-0.09
-0.07
-0.05
-0.03
-0.01
N=6
5
4
3
10^8
10^10
10^12
10^14
I (W-cm^-2)
(b)
Q
-0.05
-0.04
-0.03
-0.02
-0.01
N=8
7
6
5
10^8
10^10
10^12
10^14
I (W-cm^-2)
(c)
Q
-0.04
-0.03
-0.02
-0.01
N=10
9
8
7
10^8
10^10
10^12
10^14
I (W-cm^-2)

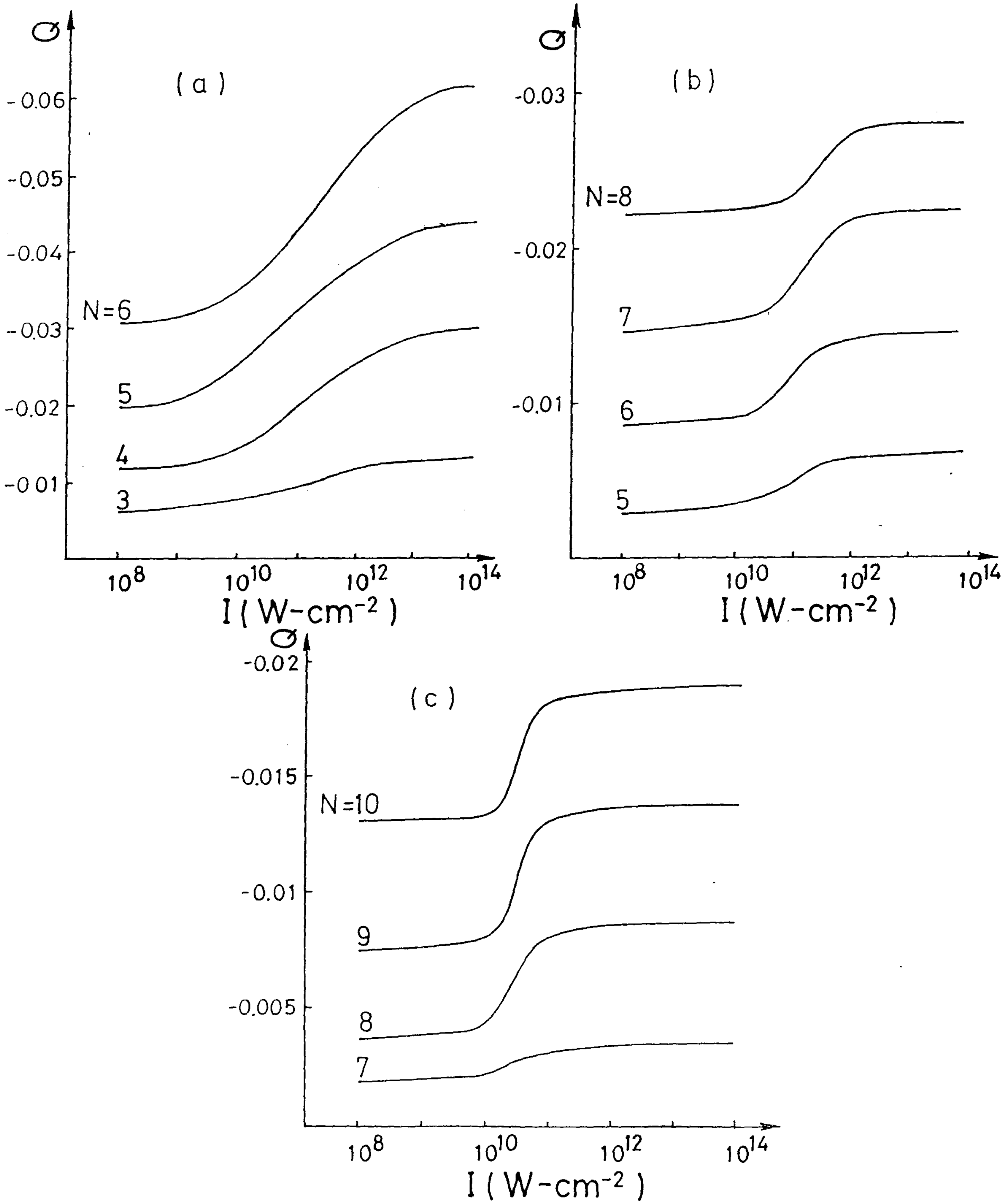

Q
(a)
-0.06
-0.05
-0.04
-0.03
-0.02
-0.01
N=6
5
4
3
10^8
10^{10}
10^{12}
10^{14}
I (W-cm^{-2})
Q
(b)
-0.03
-0.02
-0.01
N=8
7
6
5
10^8
10^{10}
10^{12}
10^{14}
I (W-cm^{-2})
Q
(c)
-0.02
-0.015
-0.01
-0.005
N=10
9
8
7
10^8
10^{10}
10^{12}
10^{14}
I (W-cm^{-2})

Fig. 7